

--SUPPORTING INFORMATION--

Experimental and Computational Investigation of Acetic Acid Deoxygenation over Oxophilic Molybdenum Carbide: Surface Chemistry and Active Site Identity

Joshua A. Schaidle^{,†}, Jeffrey Blackburn[‡], Carrie Farberow[†], Connor Nash[†], K. Xerxes Steirer[#],
Jared Clark[†], David Robichaud[†], and Daniel A. Ruddy[‡]*

[†]National Bioenergy Center, [‡]Chemistry and Nanoscience Center, and [#]Materials Science Center,
National Renewable Energy Laboratory, Golden, Colorado 80401, United States

*Corresponding Author: Joshua.Schaidle@nrel.gov

Contents

- i. Experimental Details – Mass Spectroscopy Deconvolution
- ii. Supporting Figures
- iii. Supporting Tables
- iv. Supporting References

i. Experimental Details – Mass Spectroscopy Deconvolution

Reactants and products were monitored during temperature programmed reaction (TPRxn) experiments with an online mass spectrometer (RGA 100, Stanford Research Systems). Table S1 displays the relative intensities for mass fragments of a given compound. As mass fragmentation patterns are known to be instrument specific,¹⁻³ pure compound fragmentation patterns were collected using the online MS for all compounds except ethane and were incorporated into the deconvolution algorithm. For ethane, the mass fragmentation pattern was obtained from the NIST Chemistry WebBook database.⁴

The mass fragments in Table S1 were recorded as a function of reaction temperature and corrected for overlapping signals, or deconvoluted, according to a method adapted from Zhang, et al.⁵ A system of linear equations was derived from mass conservation to solve for the corrected signals of each compound as a function of temperature and is expressed as

$$\mathbf{R} = \mathbf{C} * \mathbf{MS} \quad (\text{S1})$$

where \mathbf{R} is a matrix of N_T rows by N_i columns representing the raw mass spectral data set. Each row of \mathbf{R} is the mass spectrum at a given temperature (T) and each column corresponds to a mass-to-charge ratio (i). \mathbf{C} is a N_T by N_c matrix of corrected signals for all of the N_c compounds. \mathbf{MS} is the N_c by N_i fragmentation pattern displayed in Table S1. The system of linear equations may be solved for \mathbf{C} to obtain the deconvoluted signal for each N_c compound as a function of temperature. As a result of the linear algebra operations, each N_c compound signal in \mathbf{C} was normalized to an aggregate fragmentation pattern intensity, $F_{m,normal}$, which accounts for contributions to the compound signal from more than one mass-to-charge ratio. For example, $F_{m,normal}$ for hydrogen is equal to the normalized intensity of the primary mass fragment ($F_{m,normal} = 100$ for $m/z = 2$) whereas for acetaldehyde $F_{m,normal}$ is equal to 132.8 as a result of overlapping

signals in the fragmentation pattern, and thus multiple contributions to the compound signal. The deconvolution method was completely dependent on the fragmentation pattern, MS , and did not require any user input (e.g., primary mass fragment identification). The deconvoluted data were then corrected similarly to the method described by Ko, et al. for relative differences in ionization efficiency (I_x), quadrupole transmission (T_m), and electron multiplier gain (G_m).⁶ The ionization efficiency is primarily dependent on the number of electrons per molecule expressed as

$$I_x = 0.6 * \frac{[\# \text{ of } e^-]}{14} + 0.4 \quad (S2)$$

The gain of the electron multiplier is a function of ion mass and was calculated relative to carbon monoxide (CO)

$$G_m = \sqrt{\frac{28}{MW}} \quad (S3)$$

In addition, the quadrupole transmission is also a function of ion mass and was approximated as

$$T_m = \begin{cases} 10^{(30-MW)/155} & MW > 30 \\ 1 & MW < 30 \end{cases} \quad (S4)$$

The final correction factor (C_F) is given by

$$C_F = \frac{1}{100 * I_x} * \sum_{mass \text{ fragment}} \frac{F_m}{G_m * T_m} \quad (S5)$$

where the summation is over all mass fragments for the compound and F_m is the normalized fragmentation pattern intensity of the mass fragment. The final mass spectrum data is found by multiplying the deconvoluted data (C) by the correction factors shown in Table S2. Primary mass fragments in Table S2 were identified based on the solution to Equation S1. The primary mass fragments were considered the major fragments contributing to the respective species signal in C ,

but by no means were they considered the only contributing fragments, as the deconvoluted signals in *C* represent the complex fragmentation overlap in *MS*.

Reactant conversion during TPRxn experiments was calculated using Equation S6:

$$X_r = \left(1 - \frac{I_r}{I_{r,i}} \right) \times 100 \quad (\text{S6})$$

where X_r is the conversion of reactant r (i.e., acetic acid, acetaldehyde, ethanol, or H_2), I_r is the normalized intensity of reactant r , and $I_{r,i}$ is the initial normalized intensity of reactant r prior to the start of the TPRxn experiment. Reactant consumption rates, R , were calculated according to Equation S7:

$$R = \frac{X_r \times F_{r,i}}{m_{cat} \times N_{sites}} \quad (\text{S7})$$

where $F_{r,i}$ is the molar flow rate of reactant r at the inlet of the reactor, m_{cat} is the mass of catalyst loaded into the reactor, and N_{sites} is the active site density (sites/g_{cat}) as determined by H_2 chemisorption or NH_3 temperature programmed desorption.

ii. Supporting Figures

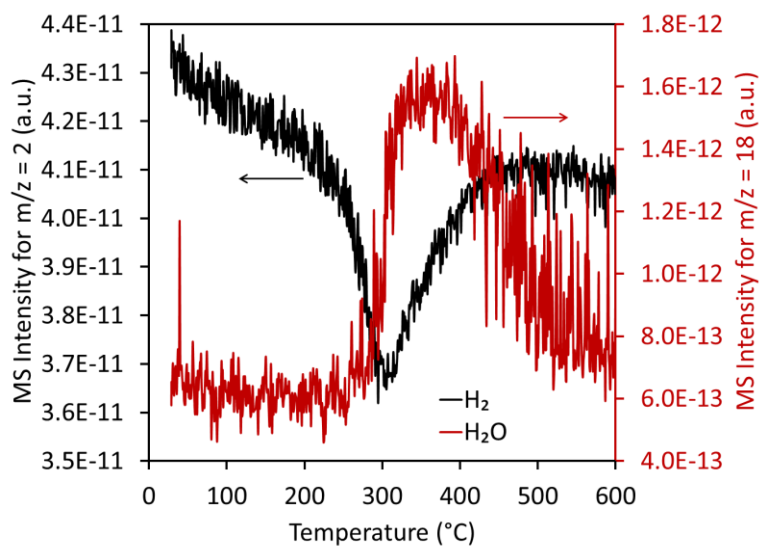


Figure S1. Consumption of H₂ and production of H₂O during a temperature programmed reduction of Mo₂C.

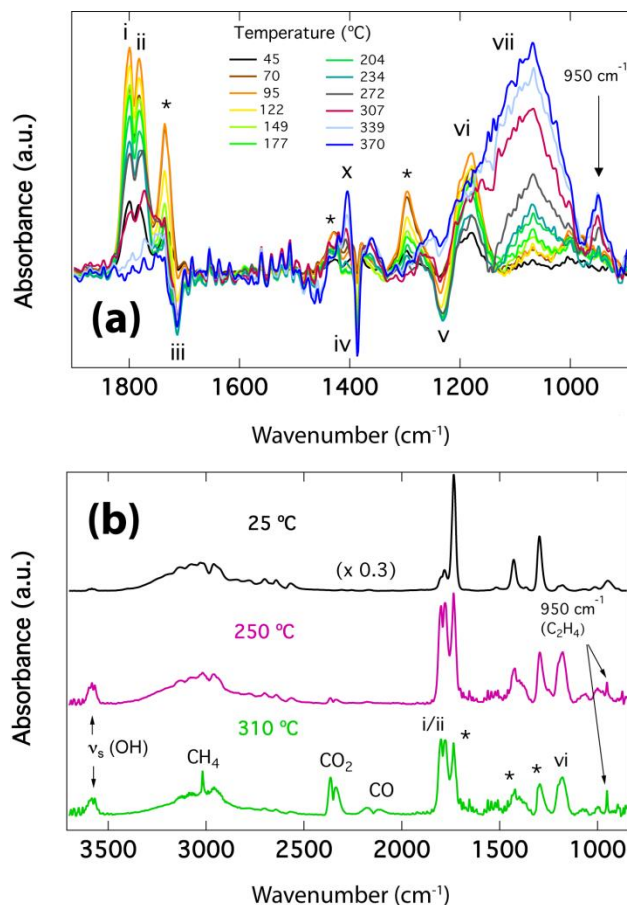


Figure S2. Temperature-dependent DRIFTS spectra for Mo₂C samples treated with acetic acid and heated in 4% H₂ in Ar. (a) Differential spectra for Mo₂C sample diluted in KBr. Baseline spectrum was the D₂-reduced Mo₂C sample. Before heating, gas-phase acetic acid was removed by evacuation for several hours. (b) Undiluted Mo₂C sample heated in 4% H₂ in Ar with a constant acetic acid overpressure. The baseline for this experiment was the sample after H₂ reduction and before acetic acid exposure. In all spectra, peaks corresponding to gas-phase or physisorbed acetic acid are labeled with asterisks and chemisorbed acetic acid adsorbates are labeled i – x. Gas-phase reaction products are labeled in (b).

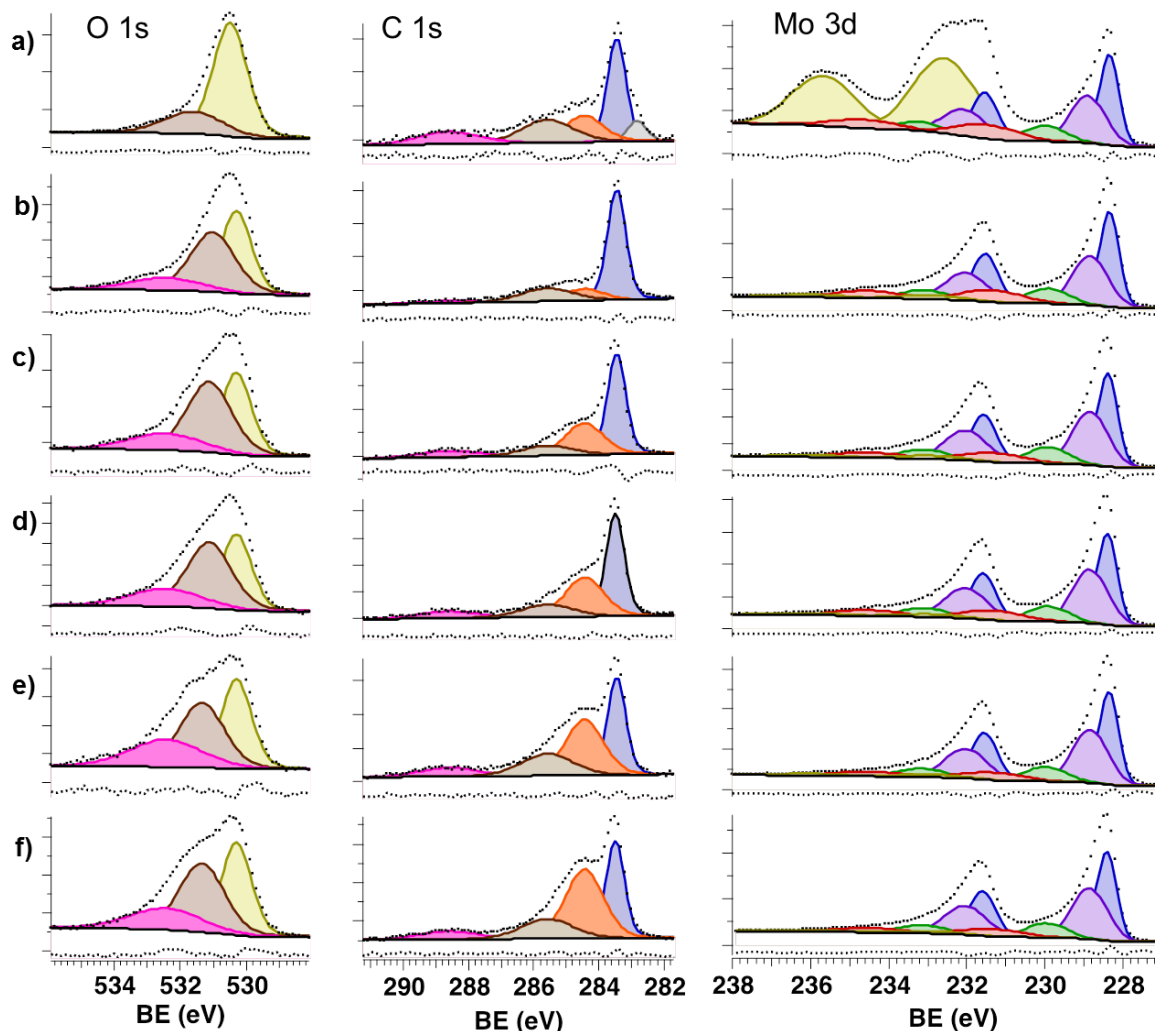


Figure S3. Core level O 1s, C 1s, and Mo 3d XPS spectra for the Mo₂C catalyst exposed to various treatments: (a) passivated (as-synthesized), (b) H₂ pretreatment at 400 °C, (c) 5 min TOS, (d) 10 min TOS, (e) 1 h TOS, and (f) 2 h TOS. Dotted line beneath spectra corresponds to the fit residual. See Table S3 for fit parameters. Reaction conditions: 50 mg catalyst, 350 °C, atmospheric pressure, 1.5 mol% acetic acid, 11 mol% H₂, and bal He (total flow rate of ca. 45.5 mL/min).

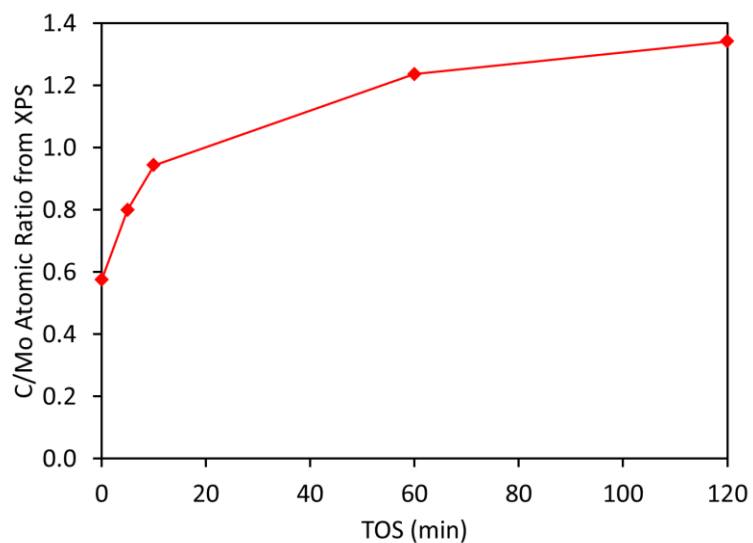


Figure S4. C/Mo atomic ratio (determined by XPS) on the surface of Mo₂C as a function of TOS. Data point at TOS = 0 min corresponds to the Mo₂C catalyst after H₂ pretreatment. Reaction conditions: 50 mg catalyst, 350 °C, atmospheric pressure, 1.5 mol% acetic acid, 11 mol% H₂, and bal He (total flow rate of ca. 45.5 mL/min).

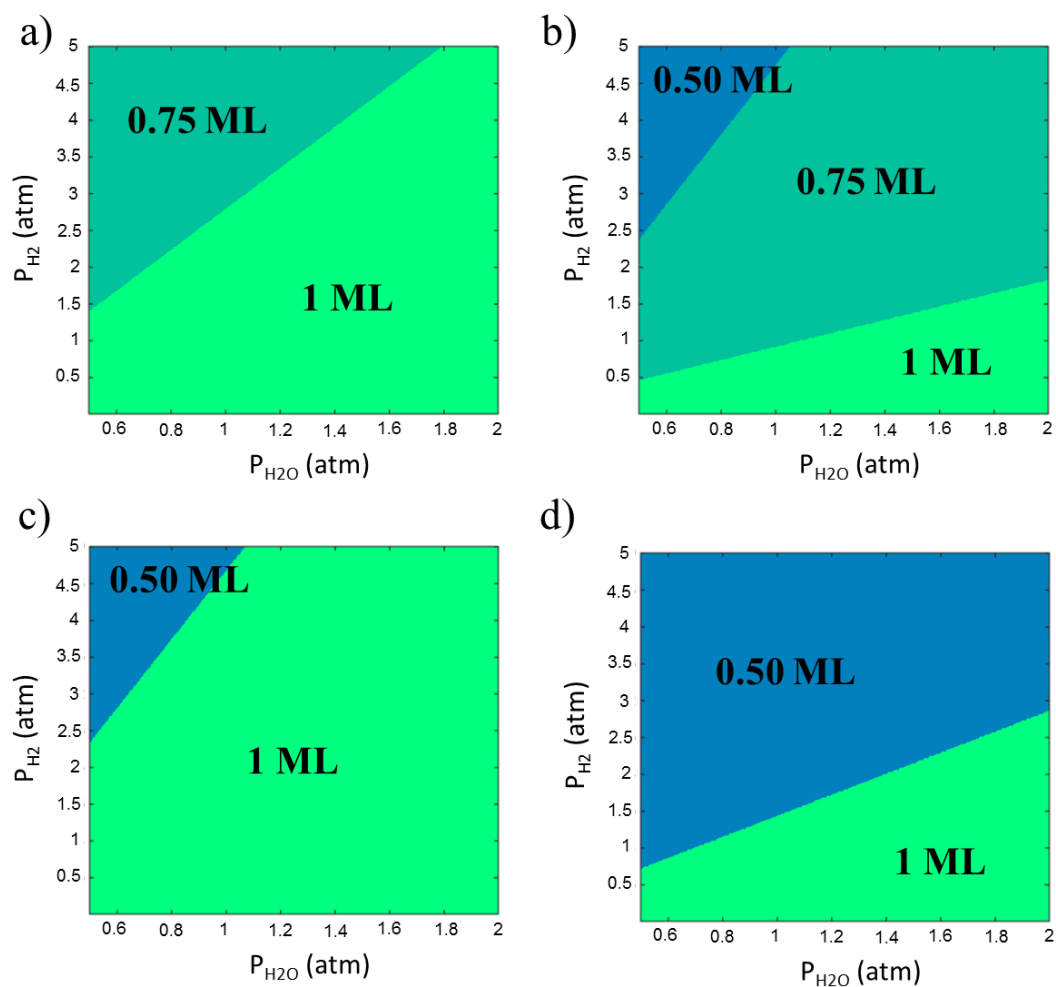


Figure S5. Phase diagrams for atomic oxygen coverage on the (a, b) Mo-terminated $\text{Mo}_2\text{C}(001)$ and (c, d) C-terminated $\text{Mo}_2\text{C}(001)$ surfaces over a range of typical *ex-situ* catalytic fast pyrolysis conditions, namely hydrogen and water partial pressures. Figures (a) and (c) were generated at a temperature of 400 °C. Figures (b) and (d) were generated at a temperature of 500 °C. 1 ML of oxygen is defined as 1 oxygen atom per each Mo surface atom on the Mo-terminated surface and 2 oxygen atoms per one C surface atom on the C-terminated surface.

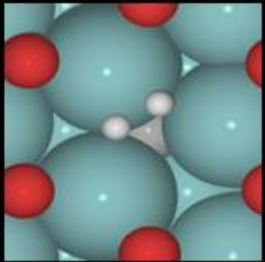
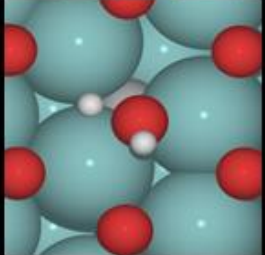
Elementary Step	Top View
$\text{H}_2^* \rightarrow 2\text{H}^*$	
$\text{H}^* + \text{OH}^* \rightarrow \text{H}_2\text{O}^*$	

Figure S6. Transition state structures for H_2 dissociation at a vacancy site on the 1 ML O/Mo-Mo₂C(001) surface and the transition state structure for water formation on the 1 ML O/Mo-Mo₂C(001) surface. Calculations were performed on a (2 x 2) unit cell.

iii. Supporting Tables

Table S1. Fragmentation patterns and relative mass fragment intensities for reactants and observed products.

Compound ^c	Mass Fragment ^{a,b}																			
	60	58	45	44	43	42	41	39	31	30	29	28	27	26	25	18	17	16	15	14
Acetic Acid	44	-	83	-	100	-	-	-	4	-	20	63	-	-	-	-	-	-	34	24
Carbon Dioxide	-	-	1	100	-	-	-	-	-	-	-	15	-	-	-	1	-	9	-	-
Acetone	-	23	1	3	100	7	3	11	-	-	5	18	7	6	1	2	-	1	24	5
Ethanol	-	-	37	3	9	3	1	-	100	6	27	34	29	17	3	4	1	1	9	5
Ethane	-	-	-	-	-	-	-	-	-	26	21	100	33	23	3	-	-	-	4	3
Acetaldehyde	-	-	3	59	33	11	5	-	1	2	100	15	5	13	5	2	1	10	66	26
Carbon Monoxide	-	-	-	-	-	-	-	-	-	-	-	100	-	-	-	1	-	2	-	-
Ethylene	-	-	-	-	-	-	-	-	-	-	2	100	59	58	11	-	-	-	1	4
Water	-	-	-	-	-	-	-	-	-	-	-	-	-	-	-	100	24	3	1	-
Methane	-	-	-	-	-	-	-	-	-	-	-	-	-	-	-	1	2	100	76	13
Helium	-	-	-	-	-	-	-	-	-	-	-	-	-	-	-	-	-	-	-	-
Hydrogen	-	-	-	-	-	-	-	-	-	-	-	-	-	-	-	-	-	-	-	-

^aThe mass fragment intensities, highlighted in bold, were identified as the primary mass fragments for each compound. ^bAll m/z values from 1 – 60 were collected during TPRxn experiments; only a selected subset is shown here corresponding to mass fragments utilized in the deconvolution algorithm. ^cMass fragmentation patterns were collected by introducing pure compound vapor into the MS for all compounds except ethane. The mass fragmentation pattern for ethane was obtained from the NIST Chemistry WebBook database.

Table S2. Correction factors and primary mass fragments for compounds of interest.

Compound	Primary Mass Fragment	Correction Factor
Acetic Acid	45	2.9
Carbon Dioxide	44	1.3
Acetone	43	1.7
Ethanol	31	2.1
Ethane	30	1.8
Acetaldehyde	29	2.8
Carbon Monoxide	28	1.0
Ethylene	26	2.1
Water	18	1.2
Methane	16	1.8
Helium	4	0.8
Hydrogen	2	0.6

Table S3. XPS fit parameters.

C 1s Model			O 1s Model			Mo 3d Model				
Peak Assignment	Peak Position (eV)	FWHM (eV)	Peak Assignment	Peak Position (eV)	FWHM (eV)	Peak Assignment	5/2 Peak Position (eV)	FWHM (eV)	Doublet Separation (eV)	Doublet Broadening (eV)
Carbide	283.5	0.68	Mo Oxide	230.3	1.07	Mo ²⁺ (Mo ₂ C)	228.4	0.60	3.18	0.2
Adventitious	284.4	1.38	Mo Oxycarbide	531.2	1.60	Mo ³⁺	228.9	1.07	3.18	0.2
Oxidative (C-O)	285.6	1.88	Hydroxyl	532.5	2.59	Mo ⁴⁺ (MoO ₂)	229.9	1.24	3.18	0.2
Oxidative (C=O)	288.6	2.20				Mo ⁵⁺	231.3	1.80	3.18	0.2
						Mo ⁶⁺ (MoO ₃)	232.9	1.90	3.11	0.0

iv. Supporting References

- (1) Ausloos, P.; Clifton, C. L.; Lias, S. G.; Mikaya, A. I.; Stein, S. E.; Tchekhovskoi, D. V.; Sparkman, O. D.; Zaikin, V.; Zhu, D. *J. Am. Soc. Mass Spectrom.* **1999**, *10*, 287-299.
- (2) Barwick, V.; Langley, J.; Mallet, A.; Stein, B.; Webb, K. *Best Practice Guide for Generating Mass Spectra*, LGC: London, U.K. 2006.
- (3) Lecchi, P.; Zhao, J.; Wiggins, W. S.; Chen, T.-H.; Yip, P. F.; Mansfield, B. C.; Peltier, J. *M. J. Am. Soc. Mass Spectrom.* **2009**, *20*, 398-410.
- (4) Stein, S. E. Mass Spectra. In *NIST Chemistry WebBook*; Linstrom, P. J., Mallard, W. G., Eds.; NIST Standard Reference Database Number 69; National Institute of Standards and Technology: Gaithersburg, 2015; <http://webbook.nist.gov>.
- (5) Zhang, Q.; Alfarra, M. R.; Worsnop, D. R.; Allan, J. D.; Coe, H.; Canagaratna, M. R.; Jimenez, J. L. *Environ. Sci. Technol.* **2005**, *39*, 4938-4952.
- (6) Ko, E. I.; Benziger, J. B.; Madix, R. J. *J. Catal.* **1980**, *62*, 264-274.